Journal of Power Sources 267 (2014) 584–597

Contents lists available at ScienceDirect

Journal of Power Sources

journal homepage: www.elsevier.com/locate/jpowsour

Coordinating plug-in electric vehicle charging with electric grid: Valley filling and target load following

Li Zhang, Faryar Jabbari, Tim Brown, Scott Samuelsen*

Advanced Power and Energy Program (APEP), University of California, Irvine, Irvine, CA 92697-3550, United States

HIGHLIGHTS

- Proposed protocol effectively fills the overnight valley.
- Computation and communication efforts are very modest.
- Modified protocol can approach a desired target load.

ARTICLE INFO

Article history:
Received 2 December 2013
Received in revised form
13 April 2014
Accepted 16 April 2014
Available online 14 May 2014

Keywords:
Plug-in electric vehicle
Grid operation
PEV charging
Decentralized control
Valley filling

ABSTRACT

Plug-in electric vehicles (PEVs) shift energy consumption from petroleum to electricity for the personal transportation sector. This work proposes a decentralized charging protocol for PEVs with grid operators updating the cost signal. Each PEV calculates its own optimal charging profile only once based on the cost signal, after it is plugged in, and sends the result back to the grid operators. Grid operators only need to aggregate charging profiles and update the load and cost. The existing PEV characteristics, national household travel survey (NHTS), California Independent System Operator (CAISO) demand, and estimates for future renewable generation in California are used to simulate PEV operation, PEV charging profiles, grid demand, and grid net load (demand minus renewable). Results show the proposed protocol has good performance for overnight net load valley filling if the costs to be minimized are proportional to the net load. Annual results are shown in terms of overnight load variation and comparisons are made with grid level valley filling results. Further, a target load can be approached in the same manner by using the gap between current load and the target load as the cost. The communication effort involved is quite modest.

1. Introduction

Plug-in hybrid electric vehicles (PHEVs) and battery electric vehicles (BEVs) are typically classified under the category of plug-in electric vehicles (PEVs) [1]. PEVs have drawn interest from government, automakers, and the public due to the potential to reduce fossil fuel consumption, tailpipe emissions, overall greenhouse gas emissions, and operating cost [2]. A variety of research papers have evaluated PEV benefits quantitatively [3–6]. The California Advanced Clean Cars programs mandates 1.4 million zero-emission and PHEVs in California by 2025 [7]. However, a consensus has been reached that one of the hurdles for large deployment (or acceptance) of PEVs is the shortage of charging infrastructure or electric vehicle supply equipment (EVSE) [8,9]. The state and local governments, as well as automakers, have shown interest in building a sufficient charging network. Previous work has presented analysis of the allocation of charging infrastructure [4,9]. There, it is shown that with large PEV penetration, even with a reliable charging network, the majority of the charging activities occur at home with the current PEV characteristics and charging rates, due to the cheap night time residential electricity and the long dwelling time needed. Furthermore, charging time strategy has been showed to have the most significant impact on charging cost reduction and overall grid operation. Here we focus on the details of coordinating PEV charging, at home, with the electric grid.

The electricity demand and generation of the grid have to be balanced at all times to assure operational stability. Charging PEVs increases the electric demand and has the potential to change the demand curve, if PEV penetration becomes significant. The time needed to charge PEVs, for most travel demands, is less than the

* Corresponding author.
E-mail addresses: gss@apep.uci.edu, gss@uci.edu (S. Samuelsen).

http://dx.doi.org/10.1016/j.jpowsour.2014.04.078
0378-7753/

Notation

t_i	time slot i in the 48-h window, e.g., 12 am–1 am, 1 am –2 am,…, 11 pm–12 am
i	time slot number, e.g., 1,2,…, 48
Δt	time slot duration, e.g. 60 min (1 h)
$\Delta t_n(t_i)$	plugged in time in time slot i for vehicle n, known
n	PEV number
ta_n	home arrival time after the last trip for PEV n
$E(t_i)$	electric demand
$D(t_i)$	electric net load
$x_n(t_i)$	charging energy at each time slot for vehicle n, decision variable
$r_n(t_i)$	maximum charging energy at each time slot for vehicle n, known
$L(t_i)$	final load with PEVs charging
T_k	time when cost is updated
V_k	vehicle number when cost updated
T_{step}	time interval for cost function updating
V_{step}	vehicle number interval for cost function updating
k	kth step to update cost function
$s_k(t_i)$	aggregated charging profile for step k
$C_k(t_i)$	cost function for charging at step k
$R(t_i)$	maximum overall charging power at each time slot, known
$X(t_i)$	overall charging load at each time slot, decision variable
$\text{TL}(t_i)$	target load
$\text{TC}_k(t_i)$	cost function for charging at step k with target load

dwelling time overnight. Unlike day time charging, overnight charging can be flexible and can be managed so that, aggregated with overall demand, it results in lower generation cost and emissions. Generally, constant (or flat) demand curves are considered beneficial for cost and environmental consideration [10]. Typically, wind and solar generation are treated as negative demand since the power cannot be controlled in the same way as other forms of generation. So the net load, total demand minus renewable generation, is targeted to be flat or at least slowly varying. The problem can be simply stated as obtaining a charging pattern so that the final net load curve has the least variation over an extended time horizon, given an original net load curve from the grid and the total charging demand for numerous PEVs.

It has become clear that if there is a significant penetration of PEVs, some form of "smart" or scheduled charging protocol will be needed. The power requirement of a large number of PEVs at peak or near peak times can lead to significant challenges in cost, delivery through grid, and even in generation and ramping capacities. This has led to several approaches to address this problem. Generally, the main goal is to schedule and shift the charging demand of the PEVs to the late evening and very early morning when the overall demand is the lowest. These are often called 'valley filling' approaches since they are aimed at leveling the overall demand to reduce the need for shutting down and restarting of large power plants. Of course, depending on specific, and relatively uncertain, costs associated with ramping and other considerations, it is possible that valley filling is not the optimal solution. For example, results in Ref. [11] show that under certain combinations of level 2 charging, station penetration, and costs assigned to ramp rates, etc., one can design a more desirable (e.g., less costly) charging profile, though how such a global plan can be realized is unclear. Here, we focus on the decentralized approach to address this challenge, as centralized approaches are difficult to implement and unlikely to be accepted.

Among the decentralized approaches that have appeared recently, paper [12] first solves a centralized optimization problem that takes into account costs associated with CO_2 generation and/or other economic and environmental costs. Based on the obtained average charging power, it then develops an algorithm that yields a decentralized implementation. Papers [13,14] use non-cooperative game concepts to develop a global valley filling protocol, under the assumption that all BEVs have similar state of charge (SOC) and other properties, and are plugged in at the same time. Paper [15] removes the homogeneity assumption and allows varied SOC, max charge rate, etc. The approaches in Refs. [13–15] are aimed at solving the global valley filling problem through a decentralized, and iterative, approach. In each iteration, a 'price' structure is communicated to the fleet of PEVs, so that each vehicle can develop an optimal (with respect to the broadcasted cost) charging profile. These profiles are sent back to the central communication node or the grid operator (e.g., the ISO – Independent System Operator), who will aggregate the total demand, based on the individual profiles, and broadcast a new price. Under relatively minor assumptions, the algorithms have convergence proofs. While the results are quite impressive, there are some challenges. Both techniques require the total number of PEVs be available for participation in the iterations needed in the optimization ([15] has results for the asynchronous case as well). Such an iterative approach might require significant communication if the number of vehicles is large. More crucially, these techniques do not ensure each PEV is charging at the maximum charging rate, which is how PEVs are currently charged. Ref. [16] attempts to address the last concern by relying on a stochastic approach in which the start of the charging period is the decision variable in the optimization problem, given the charging rate and SOC – which yields the charging duration. Under mild assumptions, the proposed iterative algorithm converges with probability one. Papers [17] and [18] propose decentralized charging controls for PHEV to avoid transformer overloading, but cannot fill the overnight demand valley. Paper [19] utilizes system-wide or nodal price for PHEV in the distribution network, however, it requires non-convex optimization solving technique.

In this paper, we focus on the similar problem with somewhat a different tack. We propose two approaches that ensure charging occurs at the maximum power, as is required with the current charging technology (1.44 kW for level 1 and 3.3 kW for level 2 EVSE), and the partial charging rate will lead to efficiency drop of the converter [20]. As a key contribution, we attempt to minimize the amount of communication needed between the large fleet of PEVs and grid operator and do not require availability of all PEVs for initiating the charging time assignments. Similar to other approaches, it can be modified to address excessive ramp rates or possible intermittent renewable sources (with some reasonable prediction window).

The basic approach can be summarized as follows. We use a cost schedule that reflects the desirable 'valley' or 'valleys' for the PEVs to charge (by assigning low costs to such periods). This is shared with individual vehicles, each solving a simple linear program to identify the periods for charging (at peak power), which will be the lowest 'cost' – and overall demand – periods. The solution is then sent back to grid operator for updating the charge structure. Note that this is not an iterative technique – there is only one set of data

transmitted each way, once. The approach uses the natural flow of PEVs in and out of the overnight (or valley) period, plus an enforced queue, and lets each vehicle sign up for a specific time period for charging. By controlling the queue (and thus the rate of communication), one can ensure the lowest cost periods (grid level valleys) are filled without solving the global valley filling problem directly.

1.1. NHTS

The vehicle travel behavior data used in this paper are derived from the 2009 National Household Travel Survey (NHTS) [21]. Several processing steps were required in order to prepare the data. In particular, data for California were selected, trips occurring without a personally owned vehicle were deleted, person-chain data were converted to vehicle-chain data, daily trips data with unlinked destinations or significant over-speed were deleted, and tours were organized into home based daily tours (first trip from home, last trip to home) [9]. A total of 20,295 vehicles were selected covering 83,005 single trips, with an average of 7.85 miles per trip and 32.13 miles per vehicle, per day.

Fig. 1 shows the histogram of the last home arrival time of the day, with 15 min (0.25 h) intervals for all those 20,295 vehicles. The peak arrivals occur in the late afternoon with almost 800 vehicles for the data set, which is around 4% of the total vehicles for this interval (around 17:00). The accumulation curve shows by 20:00, 80% vehicles have arrived and will stay until the next morning.

Fig. 1 also shows when vehicles leave home for the first trip of the day and the peak occurs in the early morning at around 7:00, by which time, 80% of vehicles have not left. Combined with the arrival time, shown in the 'Plugged in' curve, 80% of vehicles can be coordinated with the grid at home for almost half of the day, from 20:00 to 7:00 in the next day. So this time period is considered to be the most effective coordinating window between PEVs and grid.

1.2. Vehicle information

Similar to other research [11–16], this study focuses on the gird impact of macro scale of vehicle behavior where the detailed physical vehicle model was not considered; instead a parameterized vehicle operation and charging model was used. Table 1 shows vehicle parameters used in this study which were all derived from current production vehicles [22]. Gasoline price is assumed to be high enough throughout this work in order to ensure PHEVs use electricity first rather than gasoline. To simulate the future scenario, this work uses a 10% penetration of all passenger cars (PC) and light duty trucks (around 2.1 million PEVs in California) [23]. So the scaling factor from NHTS data to more than 2 million PEVs will be around 100.

Table 1
Simulation parameters for PHEVs and BEVs.

Vehicle type	MPG	kWh/mi (DC)	All-electric range (miles)	Efficiency from grid to battery	AC charging power (kW)
PHEVs	40	0.34	40	0.85	3.3
BEVs	N/A	0.31	60	0.85	3.3

1.3. Renewables and net load

The electricity sector in many countries and states have targets for meeting increasing fractions of their load demand with renewable resources to promote a shift towards a low-carbon, low-pollutant emission grid mix [10]. In California, the target is to provide 33% of all retail sales of electricity from renewable resources by the year 2020. Other states in the U.S. also aim to reach similar goals to some extent.

Fig. 2 shows the electric demand $E(t_i)$ and net load $D(t_i)$ based on wind and solar installed capacities at around 30% renewable penetration in terms of hourly resolved and monthly averaged signals. Those capacities were specified by California Public Utilities Commission (CPUC) [24]. It is well known that the demand has a diurnal pattern with a valley hours after midnight. The same pattern also can be observed for the net load for most of the days. However, as shown from day 98–99 and day 108–109, additional large peaks and valleys may also exist, in particular the relatively large valley in the afternoon. Ideally, the aggregated PEV charging profile can be used to smooth this curve as much as possible so the final load is met with lower cost and/or emissions.

To fulfill this goal, in the rest of this paper, the optimization of valley filling from the grid perspective will be first introduced to provide a reference solution. And it will introduce the mechanism

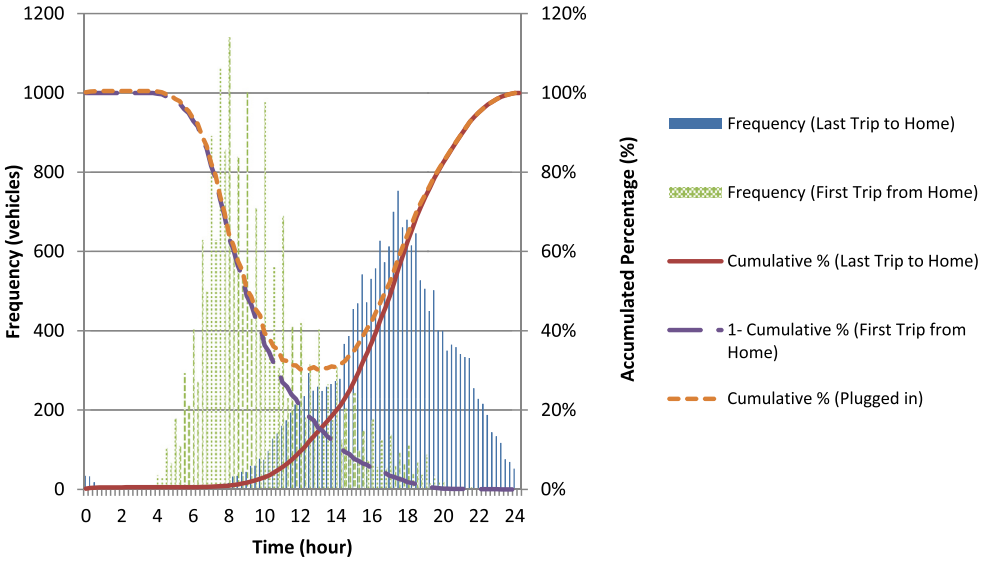

Fig. 1. Vehicles home departure and arrival time distribution and charging availability.

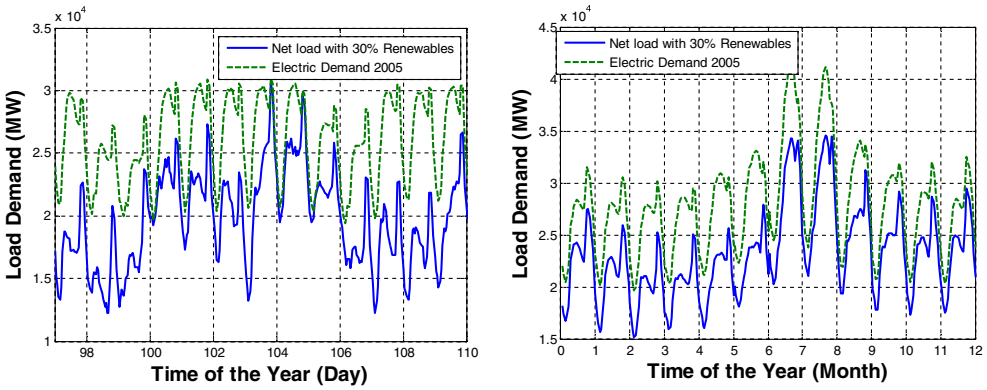

Fig. 2. Hourly resolved electric demand and net load for ten days (left) and on a monthly average basis (right).

of optimal charging from the perspective of each individual PEV as well as the protocol to update the cost function broadcast by the grid operator to achieve the optimality at the grid scale. Additionally, the year-long results will be shown and compared to the original net load and the results from grid level valley filling. Finally, a modified protocol will be introduced for the final load to approach a pre-defined target load which may not only be the solution of grid level valley filling.

2. Grid level valley filling

As mentioned earlier, the grid favors certain types of load curves, independent of the behavior of individual PEVs. Valley filling is thus a strong preference, in which ideal valley filling is to solve a convex optimization problem with the constraints on total energy consumption of PEVs. The optimization details can be formatted as follows.

$$\min \sum_i (D(t_i) + X(t_i))^2 \tag{1}$$

Subject to

$$\Delta t \times \sum_i X(t_i) = B = \sum_n b_n \tag{2}$$

where $X(t_i)$ is the overall charging power at each time slot t_i, and B is the total charging energy of all PEVs for a whole day, which is considered to be known, which the summation of the charging energy b_n for individual PEV. This problem format or the corresponding result has been seen in papers [11,13,15,25]. The well-known solution is the following

$$X(t_i) = (\lambda - D(t_i))^+ = \max\{(\lambda - D(t_i)), 0\}$$

$$\sum_i (\lambda - D(t_i))^+ = B \tag{3}$$

where λ is the height to which that the valley is filled.

However, unless all vehicles are plugged in for the whole time horizon, this solution ignores an important constraint associated with the overall charging power: the ideal valley filling result is not feasible if there are not enough PEVs plugged-in for a specific time slot according to the PEV charging availability shown in Fig. 1. Similarly, In Refs. [11], a Charge Flexibility Constraint (CFC), is added to consider the overall charging power constraint, as well. However, the Charge Flexibility Constraint indicates a sharp decrease on the maximum charging power (plugged in PEVs) from 1:00 to 6:00, which is quite different than Fig. 1. In this time period, most PEVs are at home, thus the maximum charging power should be relatively flat. Here, Fig. 1 is used to derive an additional constraint shown in Equation (4) to provide an upper bound on the overall charging

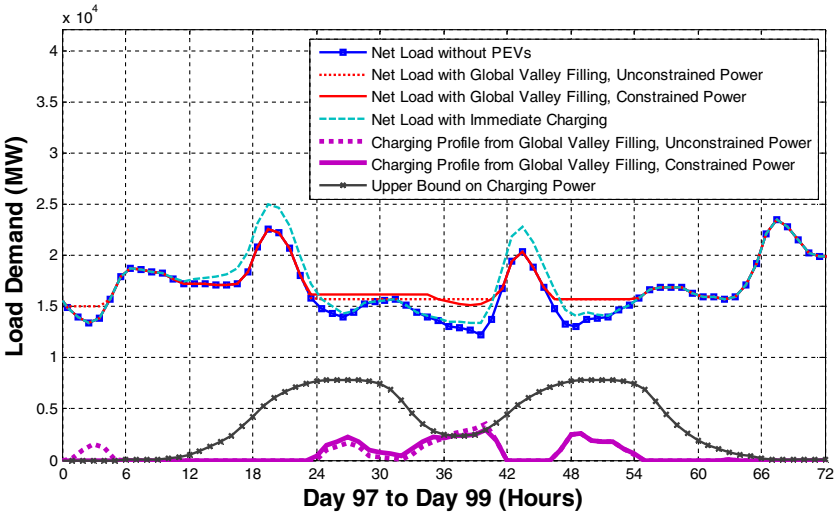

Fig. 3. Comparison of ideal valley filling results without power constraint and constrained valley filling results with power constraint.

power, depicted by the black line marked with the cross sign in Fig. 3. Essentially, $R(t_i)$ is the product of the amount of plugged in PEVs and the individual charging power (3.3 kW in this study). This constraint is independent from the electric load curve and in reality can be derived from historical plug-in and plug-out data. As contrast to the ideal valley filling without a power limit, the combination of (1) (2) (4) can be defined as constrained valley filling.

$$X(t_i) \le R(t_i) \tag{4}$$

Fig. 3 shows an example of the optimal solutions for both cases on the net loads from day 97 to day 99 (hour 0 to hour 72). It is assumed that only the PEVs that arrive in Day 97 and 98 count. Day 98 is not a typical day since the largest valley does not occur overnight but in the early afternoon (at hour 39 on the graph). The ideal valley filling result, the dotted line, requires more vehicles than are actually plugged in between hours 36–40 (i.e. arrived and plugged in). For another period from hour 1 to hour 4 on the graph, when there is not a single PEV since no vehicle has arrived, the ideal valley filling draws power from the grid as well. When the inequality constraint in Equation (4) which is represented by the black curve marked with the cross sign at the bottom of the figure is used, no power flows to PEVs before hour 6. And, the deepest valley from hour 36 to 42 ends up being filled only partially, as shown by the solid line. Although the situation of having the biggest valley in the afternoon may not happen often, it underlines the point that the ability of PEVs to alter electric load significantly may be somewhat limited to the overnight period. Although constraint (4) considers PEV availability, it is most restrictive in the early afternoon periods. During late night periods, with some of the PEVs fully charged, the real available PEV number becomes smaller than that of plugged in PEVs. Thus, during these periods, (4) overestimates the limit and is not a restrictive constraint. Fig. 3 also shows the result from the immediate charging as a benchmark, depicted by the dashed line. It increases the peaking load by 2 GW for day 97 and day 98, indicating the necessity of the coordinated charging control, such as the valley filling approach.

Naturally, a perfect valley filling solution from (1) (2) (4) may not be achievable depending on the specific shape of the net load, the availability of the PEVs, and the individual level charge needs. A complete global valley filling solution would require a problem with decision variables on the order of the PEV population, while the ideal valley filling requires a number that is on the order of time slots (as it solves the aggregate charge at each time slot). As a compromise, in this work, the optimal solution of the constrained valley filling, i.e., (1) (2) (4), is considered the reference profile. For simplicity, the constrained valley filling will be called valley filing in the rest of this paper.

3. Protocol of individual PEV charging and cost updating

The charging profile of individual PEVs is trivial compared to the grid load and only the aggregated profile has to be considered. In a decentralized scheme, every vehicle makes the best decision for its own, in terms of the overall electricity cost available to it. This section will introduce the mechanism of optimal charging for single PEVs as well as the protocol to update the cost function broadcast by the grid operator to achieve the optimality at the grid scale, to the extent possible (given the constraint on PEV availability). After that, a one-day result will be shown at different updating frequencies. Then, the communication effort will be evaluated to verify the feasibility of the proposed protocol. Finally, the year-long results will be demonstrated and compared to the original net load and the results from valley filling formatted in the previous section.

3.1. Individual PEV charging

The initial charging strategy used for individual PEVs is similar to that in Ref. [9], except that here we are focused on overnight (at home) period. In summary, given charging vehicle demand (i.e. energy), charging constraints (i.e. plugged in time window and charging power limits), charging cost (i.e. price of electricity, as provided by grid operator), each PEV finds the optimal way to charge such that its individual cost can be minimized, as shown below.

Problem formulation

1. Decision variables:

The SOC increase (or electricity recharged) of the PEV n for each time slot t_i given by $x_n(t_i)$.

2. Cost function:

The summation of the total charging cost is given by:

$$\sum_i C(t_i) \times x_n(t_i) \tag{5}$$

where $C(t_i)$ is the cost per kWh (DC) during the time t_i, derived from the electricity cost provided by grid operator.

3. Constraints:

1) The total energy charges during the home dwelling period should match the consumed energy during the day (known and fixed):

$$\sum_i x_n(t_i) = b_n \tag{6}$$

2) The lower bound on $x_n(t_i)$ is zero and for the upper bound, it is the product of the charging power at home $p_n(t_i)$ (3.3 kW), plugged in $\Delta t_n(t_i)$ time for charging in each time slot $\Delta t_n(t_i)$, and charging efficiency η (0.85).

$$0 \le x_n(t_i) \le r_n(t_i) = p_n(t_i) \times \overline{\Delta t_n(t_i)} \times \eta \tag{7}$$

If a PEV arrives home at 17:30 and leaves at 7:45 next day, and the time slot duration Δt is 1 h (60 min), then the plugged in time for charging from 17:00 to 18:00, $\Delta t(t_{18})$, is 0.5 and the plugged in time for charging from 7:00 to 8:00 in the next day, $\Delta t(t_{32})$, is 0.75.

4. Assumptions on the variables:

1) The span of plugged in time for each vehicle is fixed by the NTHS data. That is, each PEV controller knows the time for the first trip the next day.
2) The electricity cost is not exactly the same in any two time intervals, i.e., $C(t_i)$ values are distinct.
3) The charging power and AC to DC efficiency are assumed to be a constant and known.

3.1.1. Charging profile

The key is the price made available to each PEV. At specific instants (e.g., every 30 min or after every 10,000 cars have 'registered' for the night), the grid operator sends the recently arrived vehicles a price profile $C(t_i)$. We start with the simplest option: $C(t_i)$ is simply the electricity net load (i.e. demand minus renewable) $D(t_i)$. In reality, the cost must have different values at different times.

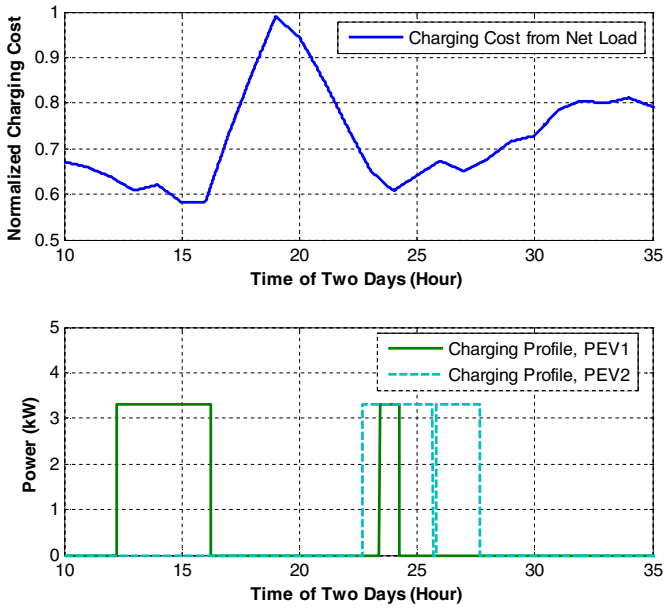

Fig. 4. Charging profiles for two PEVs with different energy requirements and plug-in window.

Since the cost for a specific time slot is different than any other, optimizing the cost function in (5) above will choose the lowest point to charge and then jump to the second lowest one with the maximum charging power until the SOC reaches 100%. In this sense, the unrealistic partial rate charging [11–15] can be avoided. Indeed, there can be at most one partial charge time period, which means the charging stops partly through that period (e.g., 15 min into the a 60 min period). The detailed proof is shown in the Appendix.

Fig. 4, lower panel, shows charging profiles for two PEVs by assuming the charging cost on the top pane, which is obtained from the net load from day 98 to day 99. The two PEVs arrive home at 5:15 and 16:40, respectively. So PEV 1 decides to charge from 12:00 to 16:00 and late in the evening to guarantee full charge. For PEV 2, the lowest cost available occurs overnight so it decides to charge then with charging turned off for about 10 min, due to the small 'bump' in price around 3 a.m. Note that this process does not prevent intermittent charging profiles, which can happen if the apparent cost to the PEV has multiple local (and similar in depth) peaks and valleys.

The intermittent charging is considered to be a milder charging condition compared to continuous charging. In this pattern, battery temperature will be lower which has less impact on degradation, since temperature is the leading factor for degradation [26–28]. Similarly, intermittency will allow the converter and other electronics to cool down. If continuous charging has to be guaranteed, an alternative algorithm can be the following: 1), each PEV calculates its required charging time at arrival; 2), depending on the departure time in the next day, the PEV finds out all the feasible continuous charging windows (i.e. charging starting points); 3), according to the electricity cost broadcast, the PEV does a simple line search to determine the optimal charging window (i.e. charging starting point). Assuming a continuous window that accommodates the needed charge exists, it is easy to see that the algorithm leads to a continuous block.

Finally, note that the communication between grid operator and PEV is quite modest: one set of prices from grid operator, one set of charging values for PEV, once.

3.2. Cost updating

Given that individual PEVs choose the lowest cost periods, the question becomes how to control/update the cost function such that the aggregated charging profile can be close to the optimum for grid operation. Intuitively, a simple approach would be based on a cost $C(t_i)$, where the original net load curve $D(t_i)$ can be used as the cost directly, as shown in the previous section. The basic scenario for cost updating is that the grid operator provides the net load forecast $D(t_i)$ each day and all PEVs will respond to the same signal.

Fig. 5 shows the final result if the same net load is shared with the total population of PHEV40 (40 miles all electric range) for a typical day. The charging load exhibits a large peak at 2:00 (26:00 on the graph) where the original net load has its minima. The incremental load is over 7 GW and lasts a short time. In this sense, the new peak will expose a significant extra burden on the grid.

As shown in the introduction, the PEVs arrival time is well distributed so the new peak above was built up through a relatively long time (more than half day) by the individual decisions made at

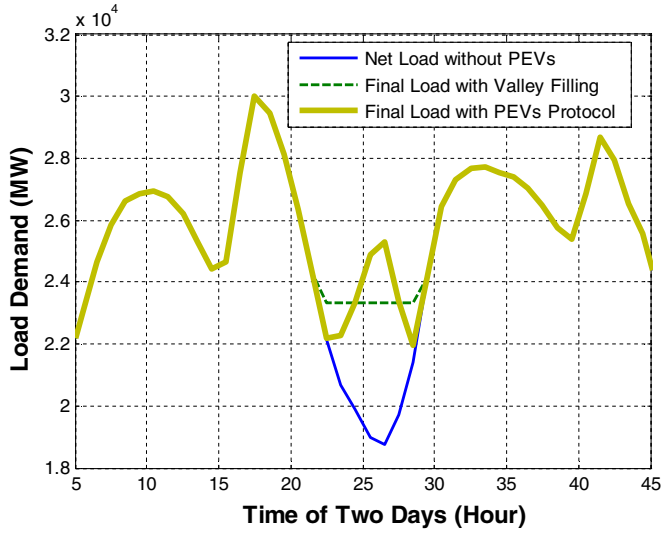

Fig. 5. Update cost function every 24 h with PHEV40 charging at 3.3 kW.

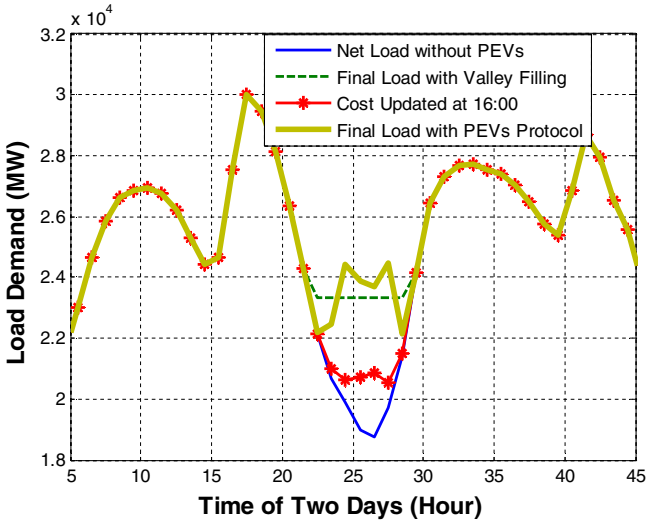

Fig. 6. Update cost function every 12 h.

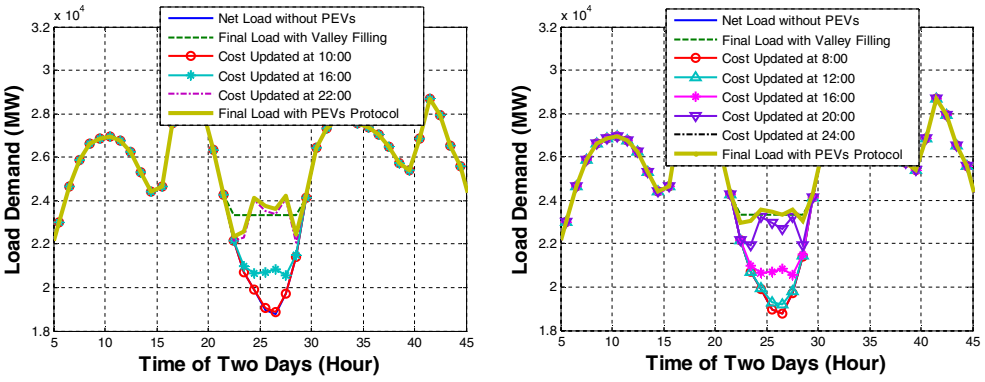

Fig. 7. Update cost function every 6 h (left) and 4 h (right).

different times. A potential solution to lower the peak is for the grid operator to change the cost function periodically so that PEVs gradually fill the valleys in the updated cost function and avoid charging at the new peak. This process can be treated as a natural valley filling.

Given that a 3.3 kW maximum load for one PEV is trivial compared to the entire grid load, the updating of the cost can be accomplished such that a number of vehicles can register, obtain prices, select charging times and communicate the results with grid operator. A typical time interval T_{step}, or a set number of PEVs V_{step}, or a set amount of the net load change in a time window (e.g., 23:00 to 6:00 in the next day) can be used to trigger the updating. Below, the protocol's details and results will be shown based on the first two methods.

1. Updating the cost function

   At each updating instant, the cost function is updated by adding the aggregated PEV charging profiles to the previous cost function.

$$C_k(t_i) = C_{k-1}(t_i) + s_{k-1}(t_i), \quad C_0(t_i) = D(t_i) \tag{8}$$

2. Profile aggregating

   As discussed before, we study the mechanism for updating the cost: fixed time internals and fixed number of vehicles.

   a. If fixed time interval is chosen, all of the individual profiles, generated from the PEVs that have arrival time, ta_n, in the interval $[T_{k-1}, T_k)$ are aggregated.

$$s_{k-1}(t_i) = \sum_n x_n(t_i) \Big/ \eta \,\forall n \quad s.t. \quad T_{k-1} \le ta_n < T_k \tag{9}$$

$$T_k = T_{k-1} + T_{\text{step}}, \quad T_0 = 4\ \text{am} \tag{10}$$

   b. If the fixed PEVs amount is chosen, each aggregation takes place with the interval of vehicle number(V_{k-1}, V_k).

$$s_{k-1}(t_i) = \sum_n x_n(t_i) \Big/ \eta \,\forall n \quad s.t. \quad V_{k-1} < n < V_k \tag{11}$$

$$V_k = V_{k-1} + V_{\text{step}}, \quad V_0 = 0 \tag{12}$$

In either case, it is important to limit the number of PEVs that will be aggregated between two cost broadcasts such that the load increment is small enough to accomplish smoothing of the overall load profile. This can be precisely controlled by T_{step} or V_{step}. In Section 3.3, the tradeoff between more frequent (more communication) and less frequent (less smooth load profile) updates will be discussed.

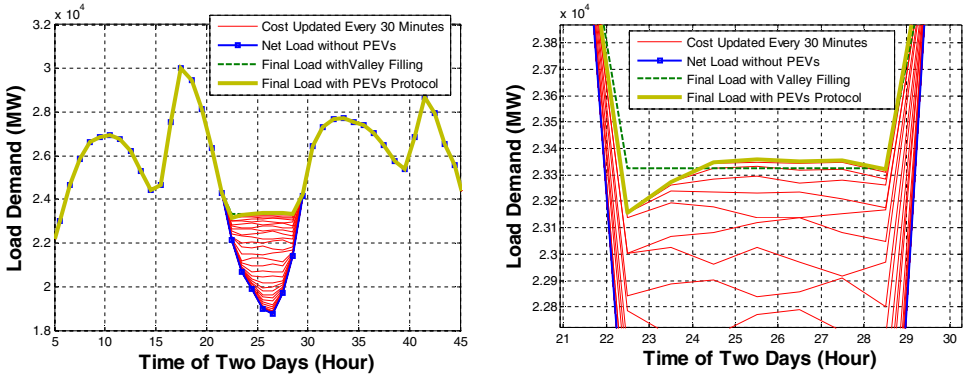

Fig. 8. Update cost function every 30 min.

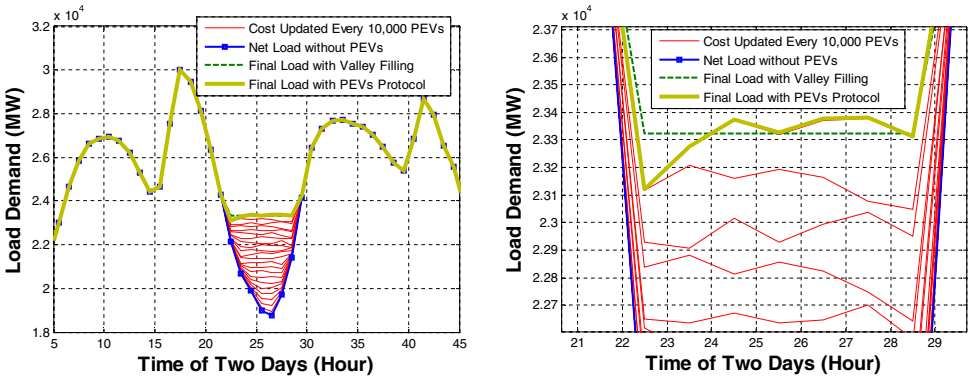

Fig. 9. Update cost function every 10,000 PHEVs.

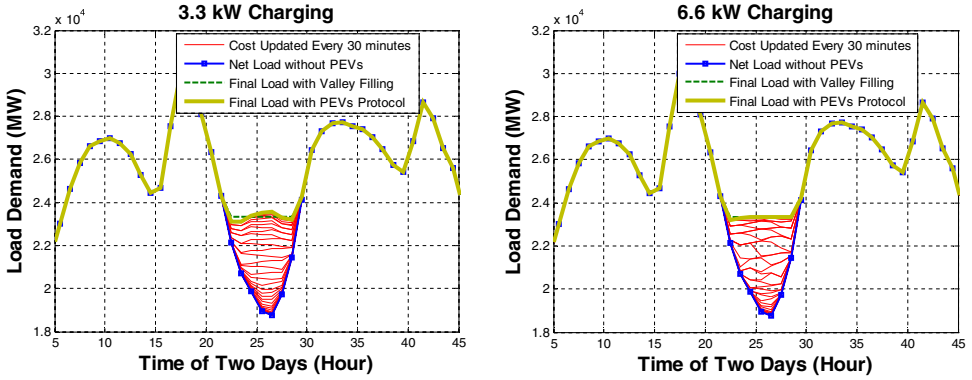

Fig. 10. Continuous charging with cost updated every 30 min for 3.3 kW (left) and 6.6 kW (right) charging power.

3.3. Protocol results and analysis

3.3.1. One-day results

Fig. 6 shows the results where T_{step} is 720 min (12 h). The increment of the net load can be divided into two parts by the line marked with the star sign, the one before 16:00 and the one after. Thus, the line shows the cost received by all the PEVs which arrive after 16:00, while the solid line was the cost received by those arriving before 16:00. As expected, the first one has the same trend as observed in Fig. 5 and the second fills the two valleys to two smaller peaks, depicted by the thick line.

Fig. 7 shows the resutls when T_{step} are 360 and 240 min (6 h and 4 h) respectively. Each curve shows the load profile (cost function) updated at the corresponding time shown in the legend. First, the final net load with PEV protocol becomes smoother with a decreased T_{step}. Second, the difference between two costs $C_k(t_i) - C_{k-1}(t_i)$ is small at the beginning which gets larger and eventually gets small again. This pattern is due to the distribution of the vehicles arrival times in Fig. 1. With the same time interval, fewer PEVs arrive home in the morning and the late evening while more PEVs arrive home in the late afternoon and early evening. That is why curves indicating costs are denser at the bottom and top, and less dense (i.e. larger change in each step) in the middle. Near the end of the process, i.e., very late evening, fewer PEV arrivals help smooth the demand curve.

As shown in Fig. 8, when T_{step} is reduced to 30 min the final curve is quite flat. The detailed examination on the right hand side indicates the variation of the curve is less than 200 MW from 23:00 to 4:00 in the next day. Thus, generators, especially load followers, can have a more steady operating condition overnight.

Another observation is the creation, and later filling, of new peaks and valleys in the cost function curve in successive steps. This is rather intuitive for this strategy. For example, all PEVs arrived between 16:00 and 16:30 are given the same cost function. They will optimize their own cost, i.e. they will try to be on where the cost is lowest. After updating, the new cost would be higher at those time slots and PEVs arriving between 16:30 and 17:00 will try to avoid charging at those time slots.

Table 2
One-day communication effort of the proposed protocol.

Result type	Update method	Max arrival (PEVs per 15 min)	Min time interval to update (minute)	Max PEVs aggregated in one update	Update times per day
Analytical (N, population)	Fixed time (T_{step})	$4\% \times N$	T_{step}	$4\% \times N/15 \times T_{step}$	$1440/T_{step}$
	Fixed PEVs (V_{step})	$4\% \times N$	$V_{step}/(4\% \times N/15)$	V_{step}	N/V_{step}
Example ($T_{step} = 30$ min, $V_{step} = 100{,}000$, $N = 2.1$ million)	Fixed time (T_{step})	84,000	30	167,000	48
	Fixed PEVs (V_{step})	84,000	18	100,000	21

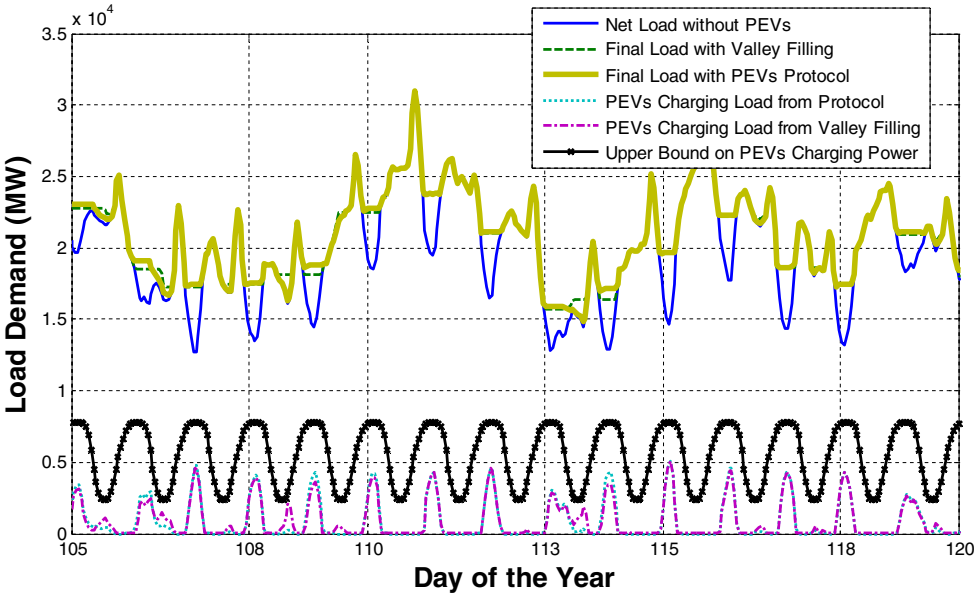

Fig. 11. Annual results from valley filling and proposed protocol with 30 min updating interval.

The fixed number of PEVs can also be used for triggering the updating of the cost (see Fig. 9) when it is preferred to control the variation of the cost in each step. Because the charging power is fixed to be 3.3 kW, the maximum change between $C_k(t_i)$ and $C_{k-1}(t_i)$ is limited by the product of charging power and the PEVs number V_{step}. In this approach, the grid operator develops a queue, as PEVs arrive, and after each V_{step} vehicles, the cost is updated and shared with the next V_{step} vehicles. In the example shown here, V_{step} is set to be 100,000 such that the maximum change on the cost can be limited to 330 MW step by step. Fig. 9 shows the results in comparison with the first method. The final variation lies within a 250 MW window from 23:00 to 4:00 in the next day. The cost function increment is more consistent and limited by 300 MW as expected in the analysis above.

As discussed earlier, continuous charging can also be guaranteed by changing the algorithm to a simple line search of the charging start point for individual PEVs. The rest of the protocol can remain the same where costs are updated by T_{step} or V_{step}. Fig. 10 shows the results of continuous charging with costs updated every 30 min, as a comparison to the results of the main protocol with intermittent charging in Fig. 9. It can be observed that the final net load with PEVs is smooth, though not as flat as the one with intermittent charging. There exists a bump in the middle of the overnight valley. This is due to the fact that the average charging time is over 3 h, for 3.3 kW power. Forcing continuous charging inevitably leads to a sizable number if PEVs having overlapping charging time, resulting in the shape seen in Fig. 10. Higher charging power would mitigate this issue. On the right hand side of Fig. 10, the results are shown with 6.6 kW charging power. As expected, the final load with PEVs is as flat as the intermittent 3.3 kW charging in Fig. 8. However, 6.6 kW charging is not likely to be popular at least in the near future because it increases the component cost, makes the distribution network less stable, and has minimal benefits in reducing the operating cost [9,29–31].

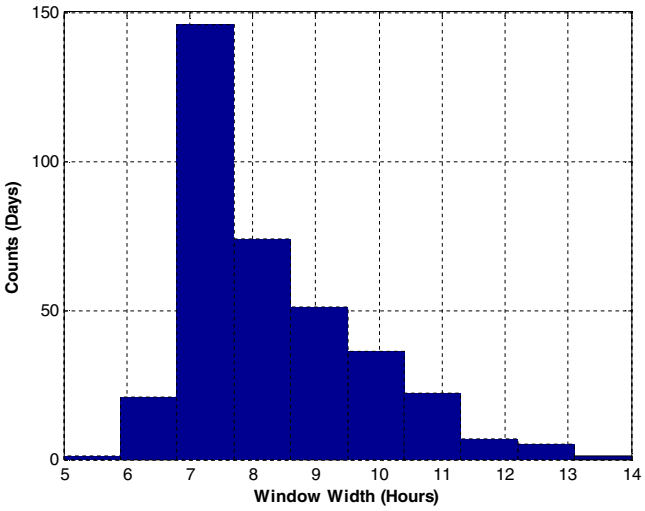

Fig. 12. Histogram of the maximum consecutive time with load varying less than 300 MW.

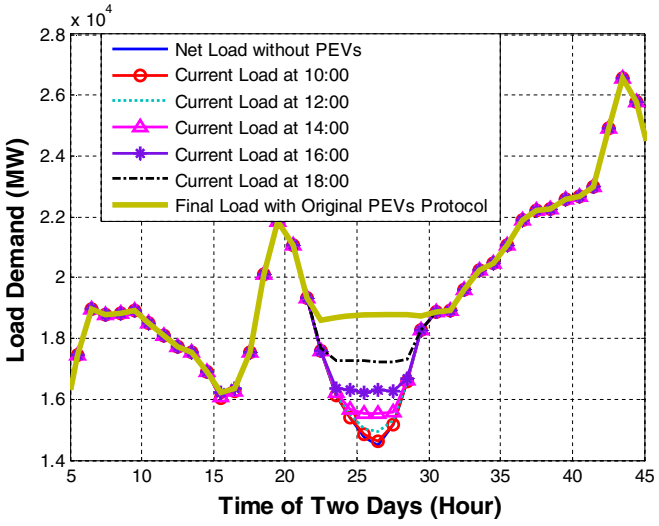

Fig. 13. Final load of the original PEVs protocol for day 108 to day 109 and loads at different times.

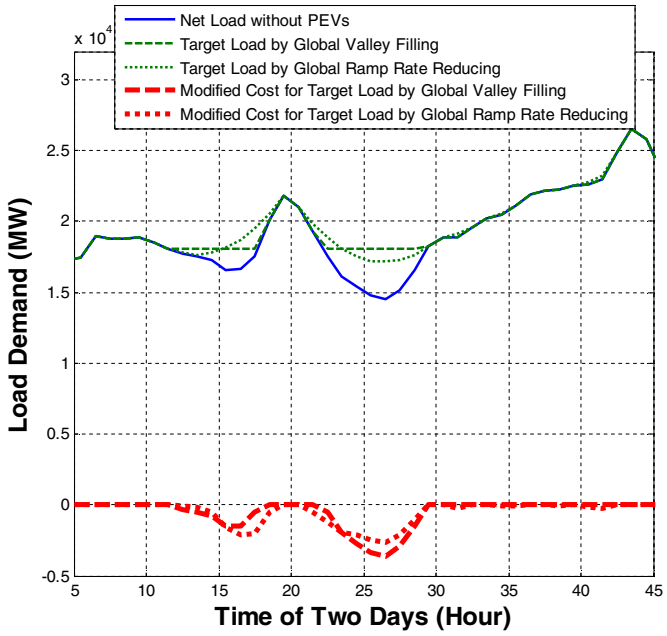

Fig. 14. Two examples of the target loads, solution of valley filling and solution of ramp rate reducing.

3.3.2. Communication effort

For the proposed protocol, either intermittent or continuous charging, each PEV receives the load curve (cost function), calculates its profile, and transmits the results one time, while the grid operator needs to receive all of the individual profiles in the set before updating. So the calculation effort is decentralized to individual PEVs while the receiving and aggregating efforts are on the grid operator, proportional to the PEVs population N. In Table 2, the amount of individual profiles received in a step and the frequency that the cost is updated are evaluated at the largest communication burden. To obtain the results shown in Fig. 8, the cost is updated 48 times per day and no more than 167,000 PEV profiles are transmitted in 30 min. As for the results in Fig. 9, the minimum updating interval is 18 min.

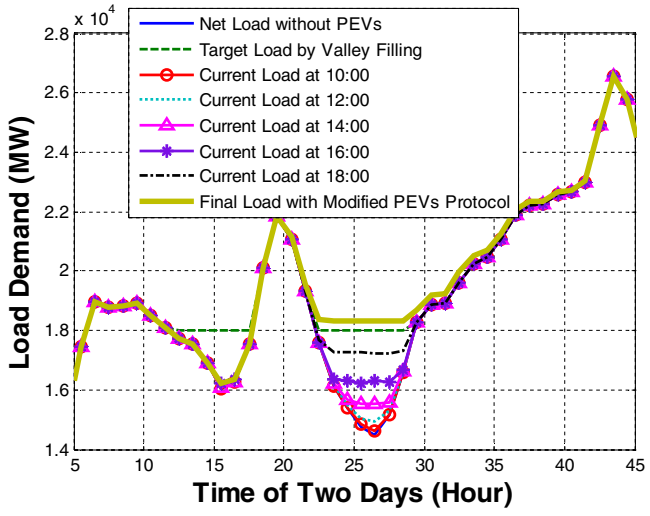

Fig. 15. Results from modified protocol without prioritizing by using the valley filling solution as the target.

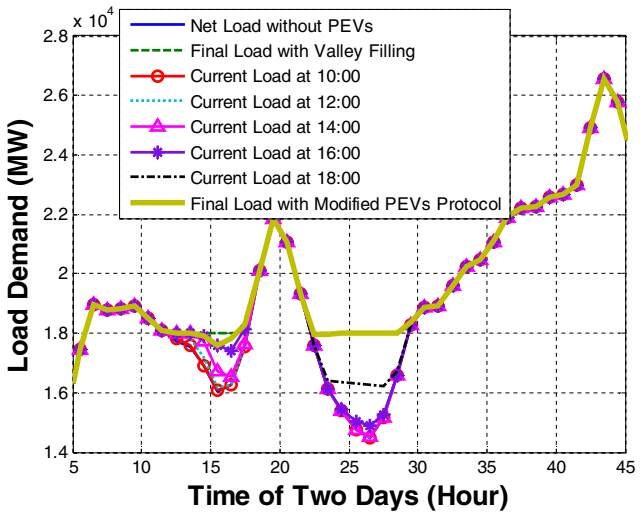

Fig. 16. Results from modified protocol with time slots 11:00 to 18:00 prioritized by using the solution of valley filling as the target.

Compared to methods in many existing publications [12–15], the calculation and communication efforts offer advantages as: 1) one linear optimization calculated and one profile transmitted at the PEV side without any global information; 2) no more than 10% of profiles are aggregated in 30 min at the operator side; 3) the cost is updated no more than 50 times per day at the operator side; 4) further, PEVs do not have to wait until a specific time to participate, which increases the potential to change the net load in late morning and afternoon.

3.3.3. Annual results

To understand the performance of the protocol for different net load curves, the same PEV charging requirements repeated each day with 30 min for T_{step} has been implemented in the simulations for the whole year. As a reference, the valley filling technique has been conducted separately. Fig. 11 is the snapshot of the results from day 105 to day 120. The charging profiles from two methods are depicted at the bottom by the dotted and dashed lines. The line marked with the cross sign shows the upper bound of the charging power, and the dashed and thick lines exhibit the final load with PEV charging.

The two charging profiles (i.e., valley filling and the protocol suggested here) are very close to each other especially when there is only one deep valley overnight. The correlation coefficient of the two profiles is 0.98 and the two resulting final loads exhibit less than 0.02% difference on the objective function in Equation (1). The only obvious difference occurs when there is another relatively deep valley in the afternoon as shown in the results from day 108–109 or day 113–114. In that case, the valley filling provides a result with two valleys filled up close to the same level while the proposed protocol does not fill the first valley in the afternoon and fills the overnight valley to a higher level. The main reason for that is the overnight valley is relatively deep, leading to a smaller cost function value so that PEVs participating in the protocol at the early steps will choose to charge overnight. When it is filled to a higher level than the afternoon, time has passed the first valley and the rest of the PEVs can still only choose overnight to charge. It needs to be noted that none of the existing research has addressed this since they require that most PEVs arrived home to initiate the protocol, often quite late in the day, e.g. midnight. Naturally, the afternoon valley cannot be filled in practice. However, for the proposed protocol in this work, one possible solution is to come up with a final

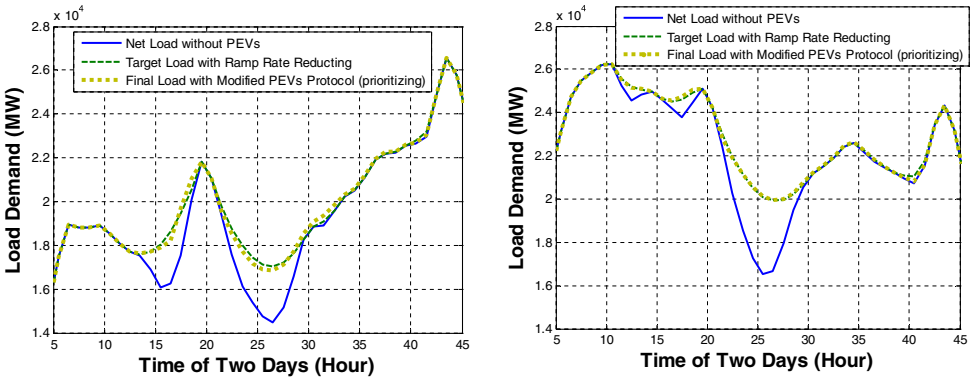

Fig. 17. Two sets of Results from modified protocol with time slots 11:00 to 18:00 prioritized by using the solution of ramp rate reducing as the target.

net load curve (e.g., the valley filling results) as a target to approach and prioritize the afternoon valley by changing the cost function. The details for this approach are discussed in Section 4.

Another important aspect, to evaluate the performance of the proposed protocol, is the final net load variations for each night. First, a maximum variation of the final load curve is defined (e.g., 300 MW). Second, the length of the consecutive time window that meets this bound is found for every night of the year. This window indicates for how long the balancing generators can operate at a relatively constant condition. Fig. 12 is the distribution of the width of this time window by setting the maximum variation to 300 MW. For most of the nights, the window width is above 7–8 h and there is only one night with a 5-h window and 21 days with a 6-h window. The widest window reaches up to 13–14 h. The widely spread distribution is due to the variety of the original net loads for different nights, shown in Fig. 11. A narrower and deeper net load valley tends to have a shorter consecutive time of flat net demand, as day 118 shows, while a wider valley is likely to have a longer consecutive time of flat demand as day 119 shows.

In summary, in the proposed protocol, each PEV calculates its own optimal profile based on the broadcast cost function which is updated frequently. The charging load of PEVs can fill the overnight valley, often to a flat final net load curve. A valley in the afternoon imposes difficulty, however, as it lies outside of the most effective charging zone, from 20:00 to 7:00 in the next day, when a large number of PEVs are plugged in.

4. Modified protocol for target load following

When there exists a relatively large valley (or multiple valleys) in the afternoon due to large solar/wind generation (or intermittent solar/wind generation), it leads to the following potential scenario: power plants have to ramp up and down quickly to meet this particular load, increasing cost and generating more emissions or, alternatively, some of the solar/wind power is curtailed. It is therefore preferable to fill or smooth the afternoon valley(s). As shown in the left pane of Fig. 13, the original protocol is not aimed at accomplishing this task and does not fill the first valley at all. As discussed in the Section 3.3.3 (Annual Results), this is due to the fact that overnight valley is more attractive than the afternoon one at the beginning. By the time the overnight valley is filled to the same level as the afternoon one, it is too late for enough PEVs to fill the first one. In order to fill the first valley, or more precisely, to approach a target load which the grid operator favors, here a modified version is built as follows: 1) grid operators define a target load by considering constraints at the grid level; 2) the cost broadcast is changed to be the current load minus the target load; 3) when appropriate, scaling is used to adjust the new cost function to ensure the desired overall charging profile. The local optimizations of individual PEVs along with the communication scheme remain the same as before. These steps will be described in detail below, followed by daily results.

4.1. Modified protocol

For the first step, a target load curve with PEVs charging, $\mathrm{TL}(t_i)$ is the summation of the known net load and the overall PEV charging load $X(t_i)$, which is unknown but bounded according to Equation (2) and inequality (4).

$$\begin{aligned} &\mathrm{TL}(t_i) = D(t_i) + X(t_i) \\ &s.t. \begin{cases} \Delta t \times \sum_i X(t_i) = B = \sum_n b_n \\ X(t_i) \le R(t_i) \end{cases} \end{aligned} \tag{13}$$

One example for the target load is to use the solution of valley filling, formed by (1) (2) (4). The solution is depicted by the dashed line in Fig. 14. Another example for the target load is the solution of ramp rate reduction, which is aimed at smoothing the final load for generation cost reduction [11]. In this study, the objective function for ramp rate reduction is shown in Equation (14), which minimizes the sum of squares of ramp rates between two consecutive time slots. The total energy and maximum power constraints associated with $X(t_i)$, in Equation (2) and (4), remain the same. The ramp rate problem consisting of (14), (2) and (4), is also a convex optimization problem and solvers, such as CVX and Quadratic Programming in MATLAB, can provide a solution fast and reliably. The solution to this problem is depicted by the dotted line in Fig. 14.

$$\begin{aligned} &\min \sum_i (\mathrm{TL}(t_{i+1}) - \mathrm{TL}(t_i))^2 = \min \sum_i ((D(t_{i+1}) + X(t_{i+1})) - (D(t_i) + X(t_i)))^2 \\ &s.t. \begin{cases} \Delta t \times \sum_i X(t_i) = B = \sum_n b_n \\ X(t_i) \le R(t_i) \end{cases} \end{aligned} \tag{14}$$

For the second step, at each time or vehicle interval, the cost function is modified by subtracting the target load from the cost function defined in Section 3.2. (i.e., the costs shown in Figs. 8 and 9). This modification, see Equation (15), results in a cost function that is essentially the gap between the current load and the target load. The current load is updated by receiving and aggregating PEV charging profiles $s_k(t_i)$ in each step exactly the same way as before while the target load is fixed. Fig. 14 also shows the initial modified cost functions for the two target loads when no PEV has arrived.

$$\begin{aligned} &\mathrm{TC}_k(t_i) = C_k(t_i) - \mathrm{TL}(t_i) \\ &C_k(t_i) = C_{k-1}(t_i) + s_{k-1}(t_i), \quad C_0(t_i) = D(t_i) \end{aligned} \tag{15}$$

Generally, the modified cost function can be non-positive if the current load is less than the target level. The wider this gap in some time slots, the more attractive it is for the PEVs to charge. By the analysis shown in the Appendix, PEVs will choose the lowest cost periods, which leads initially to late night time slots due to the largest gap between the two curves. As joining PEVs select these time slots, the gap becomes small and the magnitude reaches the same as the ones in the afternoon, PEVs will then choose to charge at the first gap. However, by then there might not be enough PEVs available to fill the first gap, as the results show in Fig. 15. It is exactly the same reason that the original protocol is not able to fill the afternoon valley in Fig. 13. Thus, an additional step of modifying the cost is needed to guarantee the afternoon gap is filled first.

For the third step, in order to prioritize the afternoon time slots, Γ, grid operator can artificially scale the costs to be more attractive than those overnight. Equation (16) shows the formulation of the modified cost $PC_k(t_i)$, that will be broadcast to PEVs, along with some requirements.

$$\begin{aligned} &PC_k(t_i) = TC_k(t_i)P(t_i) \\ &P(t_i) = 1 \,\forall\, t_i \notin \Gamma, \;\; P(t_i) > 1 \,\forall\, t_i \in \Gamma \\ &PC_k(t_i) < PC_k(t_j) \,\forall\, \{TC_k(t_i) < 0, t_i \in \Gamma, t_j \notin \Gamma\} \\ &PC_k(t_i) < PC_k(t_{i+1}) \,\forall\, \{TC_k(t_i) < 0, t_i \in \Gamma, t_{i+1} \in \Gamma\} \end{aligned} \tag{16}$$

The scaling vector, $P(t_i)$, has to be larger than one when t_i belongs to Γ, the time slots that are to be prioritized, which is 11:00 to 18:00 in the example; it can be equal to one for the rest of the time slots. Second, from 11:00 to 18:00, the scaling values need to be greater than the ratio between the depth of the overnight gap and the depth of the afternoon gap, such that the afternoon gap is filled first. The scalar must be large enough that it produces lower costs in that window, even as the afternoon gap is partially filled. Third, for the first gap, from 11:00 to 18:00, the same problem discussed earlier can exist, that early PEVs will fill the deepest point, at around 15:00, and only then the rest of the gap. When the number of PEVs is small, there is a possibility that sufficient PEVs are not available to fill the early part of the gap. $P(t_i)$, therefore, should ensure the modified function $PC_k(t_i)$ has a more negative value for the earlier time slots in the prioritized window Γ. In other words, $PC_k(t_i)$ has to have a positive slope in terms of t_i if the target has not been reached. The last line in Equation (16) is the condition required to guarantee that the gap at the earlier time slots will be filled first by the PEVs. The precise values of $P(t_i)$ were manually tuned here, through a few trials, having the value on the order of 10E6 for 11:00 and 10E3 for 18:00, and gradually decreasing exponentially.

4.2. Results and analysis

In this section, two sets of final results will be shown. First, following the above example in Fig. 15, the solution of valley filling will be used as the target load. Second, the same modified protocol will be applied on the other target, the solution of ramp rate reducing.

4.2.1. Valley filling as target

Fig. 16 shows the final load from the modified protocol with 11:00 to 18:00 prioritized. Due to the prioritizing, the gap in the small valleys is more negative than those of overnight valley, steering early arriving PEVs to toward the smaller valleys. As these are filled, or their different with the target becomes small, the updated cost function directs the PEVs to the overnight valley.

However, it ended up not filling the gap completely for the time slot 15:00 to 16:00. The reason is that the target load in the example is not feasible to achieve due to the small number of PEVs available. Note that the solution, in the dashed line, does not violate the maximum power constraint, but this constraint does not capture the actual challenge: some of the PEVs are already fully charged, so they are not able to take any more charge.

4.2.2. Ramp rate reducing as target

In Fig. 17, two 48-h net loads are shown with the left one the same as in the previous example and with the right one having multiple small valleys throughout the day. The big afternoon valley on the left pane implies substantial solar/wind generation during the day time while the two small valleys on the right pane indicate varying solar/wind generation. Compared to the example above, only the target load is changed in order to have the minimum ramp rate. The final loads with modified PEV protocol approached the targets very well. For the example on the left, the maximum difference from the target load is only 200 MW with only one exception at the time slot from 15:00 to 16:00. That difference is around 400 MW and due to the same reason mentioned before that the target is not feasible to achieve. As for the example on the right, this issue does not exist so the difference between final load and target is examined to be smaller than 200 MW for all time slots.

In summary, by slightly changing the cost function broadcast and prioritizing the time slots during the day time, the final load with PEVs can be controlled to approach a target load. To form an achievable target, grid operators need to estimate the overall charging energy in (2), maximum charging power at each time slot in (4), and other possible constraints not included here. This modified protocol extended the capability of PEVs to change the grid load from valley filling to target load following.

5. Discussion

The results presented in this work often lead to Intermittent charging. As discussed in Refs. [11,32,33], there is little evidence that intermittent charging is undesirable, indeed the avoidance of excess heating due to continuous charging over a long period, could be an important benefit. Nevertheless, if continuous charging has to be guaranteed, individual PEVs can first estimate the required charging time and then perform a line search to understand the optimal starting point such that charging cost can be minimized. The rest of the protocol for cost updating will remain the same. For the overnight valley filling, this will show a very similar result compared to intermittent charging, but have a small bump in the middle of the valley. But if charging power is doubled to 6.6 kW, the flat valley filling overnight can also be achieved.

The actual charging power for a specific PEV depends on its SOC. Generally, the maximum constant charging power is sustained before the SOC reaches 80%–90% and lower charging power is

applied until fully charged. In this study the algorithm to calculate individual charging profile does not consider the SOC dependent charging profile, but assumes maximum power can be applied all the time. However, a simple change on the algorithm can accomplish different charging profiles. For continuous charging, PEVs can estimate the SOC dependent charging profile, implement the line search to determine the charging starting point, and send back this profile. For intermittent charging, PEVs can overestimate the charging energy, implement the linear optimization to determine charging profile with constant power, tailor the end of the charging profile as the battery specifies, and send back the final profile. For the grid operator, the protocol to aggregate PEV profiles and update the cost function does not change at all.

Wind/solar power is subject to intermittency and difficult to predict [34–37]. If the forecast net load changes after most PEVs have arrived and committed, it is unlikely that any simple protocol can ensure a flat final load. In this case, a possible solution is to reschedule a certain number of PEVs. The rescheduling would require an accurate forecast of the renewable power, coupled with some ranking and identifying PEVs with flexibility to be rescheduled. Such an approach would require significant extra communication and is beyond the scope of this paper, which is focused on simple protocols with minimal communication.

The issue of the actual cost of energy, charged to the customer, by the utility is also not investigated. If the protocol is focused on overnight charging, a low uniform pricing policy is likely, though secondary valleys (reflecting intermittent renewables) may lead to more complex pricing models. Another issue, not directly addressed, is possible distribution constraints, particularly for the residential transformer, given that the data used reflect statewide numbers. The concept here can be used in relatively small networks and grids, with little to no modifications. Finally, we do not consider vehicle-to-grid (V2G) operation. While theoretically, the optimization can be modified to accommodate negative charging, such an option would entail a variety of new constraints and conditions (e.g., regarding grid stability, etc.) that are well beyond the scope of this work, as well as near term possible technologies.

6. Conclusions

Realistic electric demand from CAISO for 2005 and solar and wind power under 30% renewable penetration assumptions were used to generate the net load profile for the state of California. The 2009 National Household Travel Survey data and parameterized PEVs operating and charging model were used to simulate the charging demand and constraints with 2.1 million PEVs (10% penetration). Optimization on the aggregated profile was formed in terms of valley filling and ramp rate reducing. Optimization on individual PEV charging was formed, as well, for the objective of minimizing charging cost. Two methods on cost function updating were performed along with results for both daily and annual basis. The proposed protocol in this work shows a promising result in terms of overnight valley filling and target load approaching. Based on the data, model and results above, the following conclusions can be drawn:

1. At the demonstrated renewable penetration, the net load curve shows the biggest valley almost every night. The most effective time for charging is the window from 20:00 to 7:00 in the next day, corresponding to the availability of 80% of the total number of vehicles. With significant PEV market penetration (10%) shown in this work, coordination between individual PEVs and the grid has to be made to avoid additional and prohibitively expensive peak power periods.
2. Using grid load directly as the cost function and updating it frequently enough, by either a fixed time interval or vehicle amount, will lead to a flat final net load overnight for a relatively large time window. Updating the cost function every 30 min results in less than 300 MW variations on the final load during more than 7 h, for 90% of the days in a year. Also, the correlation of the aggregated charging loads from grid level valley filling and the proposed protocol is greater than 0.98.
3. The computation and communication efforts required by the proposed protocol are more modest than the existing works which require, potentially a large number of, iterations. Each PEV needs to compute its charge profile only once, performing a simple linear optimization problem. It also needs to send the charging profile back to the grid operator, where individual profiles are aggregated and loads are updated periodically.
4. Using the gap between the current load and final target load as the modified cost function and prioritizing the earlier time slots if necessary, a desired target net load can be approached similar to overnight valley filling.

Acknowledgment

The authors would like to thank Brian Tarroja from University of California, Irvine, for providing data on grid demand and renewable power.

Appendix

Here we present the main properties of the optimization algorithm in (5)–(7). Each PEV will minimize its costs associated the following cost function.

$$\sum C(t_i)x(t_i)$$

Subject to

$$\begin{cases} \sum x(t_i) = b \\ x(t_i) \geq 0 \\ x(t_i) \leq r(t_i) \end{cases}$$

The Lagrangian is

$$\mathscr{L} = C^T x - \nu\left(\sum x(t_i) - b\right) - \lambda^T x + \mu^T(x - r)$$

Applying the standard approach, KTT condition (which are both necessary and sufficient due to convexity)

$$\frac{\partial \mathscr{L}}{\partial x} = C(t_i) - \nu - \lambda(t_i) + \mu(t_i) = 0$$

$$\nu\left(\sum x(t_i) - b\right) = 0$$

$$\lambda(t_i)x(t_i) = 0$$

$$\mu(t_i)(x(t_i) - r(t_i)) = 0$$

From

$$\lambda(t_i)x(t_i) = 0 \rightarrow \lambda(t_i) = 0 \text{ or } x(t_i) = 0$$

Since we are only interested in charging time, we consider

$$x(t_i) \neq 0$$

Then

$$\lambda(t_i) = 0$$

Then the KTT conditions become to

$$\begin{cases} C(t_i) - \nu + \mu(t_i) = 0 \\ \nu(\sum x(t_i) - b) = 0 \\ \mu(t_i)(x(t_i) - r(t_i)) = 0 \end{cases}$$

If

$$\mu(t_i) \neq 0 \rightarrow x(t_i) = r(t_i)$$

i.e., charging at maximum power. If

$$\mu(t_i) = 0 \rightarrow x(t_i) \text{can be different than } r(t_i) \text{ but } C(t_i) = \nu$$

So the KTT condition shows either $x(t_i) = r(t_i)$ or $C(t_i) = \nu$.

If $C(t_i)$'s are distinct, then $\mu(t_i) = 0$ is possible for one time slot only, since there is only one ν.

This shows that all other $x(t_i)$'s are at maximum value with possible exception of 1.

Claim: assuming distinct prices for each time slot, the algorithm above picks the lowest cost time slots. Furthermore, the partial time slot has the highest price among time slots used (but lower than those not used).

Proof: We start with the first part of the claim. We use the following notation for the charging and non-charging time slots, respectively

$$\mathrm{I}_c = \{j | x(t_j) \neq 0\}$$

$$\mathrm{I}_{nc} = \left\{ j^{'} | x\left(t_{j^{'}}\right) = 0 \right\}$$

From the main property of the optimization in (6)–(8), for all $j \in \mathrm{I}_c$, we have $x(t_j) = r(t_j)$ except at most one; i.e., maximum charge in all time slots with at most one partial charge.

Now assume there exists some $j^{'} \in I_{nc}$ such that $C(t_{j^{'}}) < C(t_k)$ for some $k \in I_c$; i.e., one of the time slots with no charge has lower price than at least one of the charging times slots. Then consider the following:

$$C\left(t_{j^{'}}\right)\varepsilon + C(t_k)(x(t_k) - \varepsilon) = \left[C\left(t_{j^{'}}\right) - C(t_k)\right]\varepsilon + C(t_k)x(t_k) < C(t_k)x(t_k)$$

i.e., shifting the charging to the $t_{j^{'}}$ time slot reduces the cost, which is not possible as it contradicts the optimality of the solution. This shows the optimized solution picks the lowest cost time slots.

For the last part of the claim, we follow the same logic: suppose t_j was associated with partial charging, i.e., $x(t_j) < r(t_j)$. Suppose there exist t_k such that $C(t_j) < C(t_k)$ and $x(t_k) = r(t_k)$. Clearly, there exists $\varepsilon > 0$ small enough such that

$$\begin{cases} 0 < x(t_j) + \varepsilon \leq r(t_j) \\ 0 \leq x(t_k) - \varepsilon < r(t_k) \end{cases}$$

Similar to above, we note that

$$\begin{aligned} &C(t_j)(x(t_j) + \varepsilon) + C(t_k)(x(t_k) - \varepsilon) \\ &= [C(t_j) - C(t_k)]\varepsilon + C(t_j)x(t_j) + C(t_k)x(t_k) \\ &< C(t_j)x(t_j) + C(t_k)x(t_k) \end{aligned}$$

which means shifting from t_k to t_j reduces the cost, which contradicts optimality of the solution, implying that $C(t_j) > C(t_k)$ for all $\{k \neq j | k \in \mathrm{I}_c\}$..

References

[1] SAE Hybrid – EV Committee, Hybrid Electric Vehicle (HEV) & Electric Vehicle (EV) Terminology, SAE, 2008.
[2] Mehrada Ehsani, Yimin Gao, Ali Emadi, Modern Electric, Hybrid Electric, and Fuel Cell Vehicles: Fundamentals, Theory, and Design, 2004.
[3] Karel H. Jansen, Tim M. Brown, G. Scott Samuelsen, J. Power Sources 195 (2010) 5409–5416.
[4] Li Zhang, Tim Brown, G. Scott Samuelsen, J. Power Sources 196 (2011) 6559–6566.
[5] E.D. Tate, Peter J. Savagian, The CO_2 Benefits of Electrification E-REVs, PHEVs and Charging Scenarios, in: SAE World Congress & Exhibition, SAE, 2009.
[6] Stephanie Stockar, Pinak Tulpule, Vincenzo Marano, Giorgio Rizzoni, Energy, Economical and Environmental Analysis of Plug-In Hybrids Electric Vehicles Based on Common Driving Cycles, in: 9th International Conference on Engines and Vehicles, SAE, 2009.
[7] California Air Resources Board, Advanced Clean Cars Program, C.A.R. Board, 2012.
[8] M. Yilmaz, P. Krein, IEEE Trans. Power Electron 28 (2013) 2151–2169.
[9] Li Zhang, Tim Brown, Scott Samuelsen, J. Power Sources 240 (2013) 515–524.
[10] Joshua D. Eichman, Fabian Mueller, Brian Tarroja, Lori Smith Schell, Scott Samuelsen, Energy (2013).
[11] Keenan Valentine, William G. Temple, K. Max Zhang, J. Power Sources 196 (2011) 10717–10726.
[12] Changsun Ahn, Chiao-Ting Li, Huei Peng, J. Power Sources 196 (2011) 10369–10379.
[13] Zhongjing Ma, Duncan Callaway, Ian Hiskens, Decentralized charging control for large populations of plug-in electric vehicles, in: 49th IEEE Conference on Decision and Control (CDC), IEEE, 2010, pp. 206–212.
[14] Zhongjing Ma, Ian Hiskens, Duncan Callaway, A Decentralized MPC Strategy for Charging Large Populations of Plug-in Electric Vehicles, Preprints of the 18th IFAC World Congress Milano (Italy), August, 2011.
[15] Lingwen Gan, U. Topcu, S. Low, Optimal decentralized protocol for electric vehicle charging, in: 50th IEEE Conference on Decision and Control and European Control Conference (CDC-ECC), 2011, pp. 5798–5804.
[16] Lingwen Gan, Ufuk Topcu, Steven H. Low, Stochastic distributed protocol for electric vehicle charging with discrete charging rate, in: 2012 IEEE Power and Energy Society General Meeting, IEEE, 2012, pp. 1–8.
[17] Alexander D. Hilshey, Pooya Rezaei, Paul DH. Hines, J. Frolik, Electric vehicle charging: transformer impacts and smart, decentralized solutions, in: 2012 IEEE Power and Energy Society General Meeting, IEEE, 2012, pp. 1–8.
[18] Moein Moeini-Aghtaie, Ali Abbaspour, Mahmud Fotuhi-Firuzabad, Payman Dehghanian, PHEVs centralized/decentralized charging control mechanisms: requirements and impacts, in: 2013, IEEE North American Power Symposium (NAPS), 2013, pp. 1–6.
[19] M. González Vayá, Göran Andersson, Centralized and decentralized approaches to smart charging of plug-in vehicles, in: 2012 IEEE Power and Energy Society General Meeting, IEEE, 2012, pp. 1–8.
[20] Kazuhiro Kondo, Koichi Kojima, Mamoru Sasaki, Development of Charging System for Plug-in Hybrid Vehicles, EVS26, Los Angeles, California, 2012.
[21] Federal Highway Administration, The U.S. Department of Transportation, Introduction to the 2009 National Household Travel Survey (cited). Available from: http://nhts.ornl.gov/introduction.shtml.
[22] U.S. Department of Energy, Chevrolet Volt Fuel Economy, 2012 (cited 2012). Available from: http://www.fueleconomy.gov/feg/Find.do?action=sbs&id=31618.
[23] CARB California Air Resource Board, EMFAC, 2007.
[24] Paul Douglas, E. Stoltzfus, A. Gillette, J. Marks, California Public Utilities Commission, 2009.
[25] Paul Denholm, Michael Kuss, Robert M. Margolis, J. Power Sources 236 (2013) 350–356.
[26] Scott B. Peterson, Jay Apt, J.F. Whitacre, J. Power Sources 195 (2009) 2385–2392.
[27] Saeid Bashash, Scott J. Moura, Joel C. Forman, Hosam K. Fathy, J. Power Sources 196 (2010) 541–549.
[28] John Wang, Ping Liu, Jocelyn Hicks-Garner, Elena Sherman, Souren Soukiazian, Mark Verbrugge, Harshad Tataria, James Musser, Peter Finamore, J. Power Sources 196 (2011) 3942–3948.
[29] Robert C. Green Ii, Lingfeng Wang, Mansoor Alam, Renew. Sustain. Energy Rev. 15 (2011) 544–553.
[30] L. Fernandez Pieltain, T.G.S. Roman, R. Cossent, C.M. Domingo, P. Frias, IEEE Trans. Power Syst. 26 (2011) 206–213.
[31] Michael Kuss, Tony Markel, William Kramer, 2010.
[32] B.K. Purushothaman, U. Landau, J. Electrochem. Soc. 153 (2006) A533–A542.
[33] Jun Li, Edward Murphy, Jack Winnick, Paul A. Kohl, J. Power Sources 102 (2001) 302–309.
[34] Ma Lei, Luan Shiyan, Jiang Chuanwen, Liu Hongling, Zhang Yan, Renew. Sustain. Energy Rev. 13 (2009) 915–920.
[35] Ronan Doherty, Mark O'Malley, Quantifying reserve demands due to increasing wind power penetration, in: 2003 IEEE Bologna Power Tech Conference Proceedings, vol. 2, IEEE, 2003, p. 5.
[36] Yuri V. Makarov, Pavel V. Etingov, Jian Ma, Zhenyu Huang, Krishnappa Subbarao, IEEE Trans. Sustain. Energy 2 (2011) 433–442.
[37] Yuri V. Makarov, Clyde Loutan, Jian Ma, Phillip de Mello, IEEE Trans. Power Syst. 24 (2009) 1039–1050.